Acta Cryst. (1975). B**31**, 2405

The Crystal Structure of Nasinite, $Na_2[B_5O_8(OH)].2H_2O$

By E. Corazza, S. Menchetti and C. Sabelli

Centro di Studio per la Mineralogia e la Geochimica dei Sedimenti, Istituto di Mineralogia dell'Università,
50121 *Firenze, Italy*

(*Received* 20 *January* 1975; *accepted* 29 *March* 1975)

The crystal structure of synthetic nasinite, $Na_2[B_5O_8(OH)].2H_2O$, has been determined and refined from 1320 single-crystal diffractometer data by means of direct methods and least-squares refinement with anisotropic thermal parameters (isotropic for hydrogen atoms), giving $R=0.027$. Hydrogen atoms were located on a ΔF map. Lattice constants determined on the same diffractometer are: $a=12.015$ (2), $b=6.518$ (1), $c=11.173$ (1) Å; space group $Pna2_1$; $Z=4$. The structure is dominated by sheets in the **bc** plane, resulting from polymerization of $[B_5O_8(OH)]^{2-}$ polyions. Both Na atoms are eightfold coordinated; one is located on the B–O sheet, the other between the hexagonal rings protruding alternately in the space between the sheets. The Na polyhedra framework is three-dimensional and provides links between B–O sheets. Additional inter-sheet connexions are provided by H bonds from the OH group and from one of the water molecules. The structure closely resembles that of $K_2[B_5O_8(OH)].2H_2O$; comparisons with this compound are made.

Introduction

Of the several phases obtained in the Na_2O–B_2O_3–H_2O system under hydrothermal conditions at 150 °C (Stoppioni, 1974), the present compound was already known as the mineral nasinite (Cipriani & Vannuccini, 1961; Cipriani, 1961). The one reported by these authors is up to now the only natural occurrence of the mineral, which was found in the geothermal field of Larderello, Tuscany (Italy) associated with other borates and particularly with biringuccite.

There has been discussion about the chemical formula of nasinite, known also as 'Auger's borate'. In their study on the stability of ezcurrite Milman & Bouaziz (1965) recognized a phase corresponding to $2Na_2O.5B_2O_3.5H_2O$. Nies & Hulbert (1967) synthesized the same 2:5:5 phase that they identified as corresponding to nasinite, after correction of the water content, on the basis of the X-ray powder pattern. The same conclusion had been reached also by Nies & Erd (1963).

The present structural determination, from which the crystal-chemical formula $Na_2[B_5O_8(OH)].2H_2O$ results, allows nasinite to be classified among the phylloborates with three triangles and two tetrahedra as the repeat unit instead of the inoborates, as Tennyson (1963) concluded on the basis of data then available. Even the supposition that nasinite is the monoclinic dimorph of ezcurrite is to be reconsidered in view of the new results. In fact nasinite has a chemical composition different from that of ezcurrite (Cannillo, Dal Negro & Ungaretti, 1973), $Na_2[B_5O_7(OH)_3].2H_2O$, corresponding to the 2:5:7 molar ratio.

Experimental

Synthetic nasinite was prepared at 150±5°C in the range of molar $Na_2O:B_2O_3$ ratios from 0·189 to 0·415, under hydrothermal conditions, by means of a pressure vessel supplied with temperature regulation and pressure read-out. Even runs of a few hours always yielded well formed crystals up to 1 mm in size, transparent and colourless, embedded in a viscous amorphous mass. The crystals could easily be separated from the glassy part merely by rinsing, since nasinite is insoluble in cold water. The crystals sometimes show a prismatic habit elongated along [001], but mostly they are in the shape of thin pseudohexagonal plates, {100} being the prevailing form.

Identity of the synthetic compound with the mineral was confirmed by some optical and morphological characters, by the $Na_2O:B_2O_3$ ratio, and especially by the close similarity of X-ray powder patterns. Crystal data are reported in Table 1. The specific gravity was measured by flotation in a bromonaphthalene–bromoform mixture; the agreement with the calculated value for four formula units in the cell is good.

Table 1. *Crystal data*

Formula	$Na_2[B_5O_8(OH)].2H_2O$
F.W.	281·07
Space group	$Pna2_1$
Unit-cell dimensions	$a=12.015$ (2) Å
	$b=6.518$ (1)
	$c=11.173$ (1)
V	875·0 Å^3
Z	4
D_m	2·12 g cm^{-3}
D_x	2·134 g cm^{-3}
μ (Mo $K\alpha$)	3·05 cm^{-1}
$F(000)$	560

The lattice parameters were determined from the scattering angles of 25 high-angle reflexions, measured with Mo $K\alpha$ radiation on a Philips single-crystal diffractometer.

Systematic absences $k+l=2n+1$ in $0kl$ and $h=2n$

+1 in $h0l$ indicate the space groups $Pna2_1$ and $Pnam$. The non-centrosymmetric space group was chosen because of indications from the statistical test by Karle, Dragonette & Brenner (1965); the structural analysis confirmed the non-centrosymmetric space group.

Intensity data were collected on a Philips computer-controlled diffractometer (Centro di Cristallografia Strutturale del C.N.R., Pavia, Italy) from a small fragment of a crystal with Mo $K\alpha$ radiation and the ω–2θ scan technique. Up to three scans were carried out for lower intensities, each peak being integrated for 40 s and the background being measured on both sides of the peak. Reflexions with $(I_{\text{peak}}-2\sqrt{I_{\text{peak}}})\le I_{\text{back}}$ were considered as unobserved. Of 1320 reflexions scanned within the range $0{\cdot}05<\sin\theta/\lambda<0{\cdot}70$, 1199 were considered to be actually observed and were used in the structure analysis. Intensities were converted into structure amplitudes by application of the Lorentz-polarization factor appropriate to monochromatic radiation. Because of the low coefficient and the small size of the crystal no absorption correction was applied.

Table 2. *Initial phase assignments* (*MULTAN*)

h k l	$\lvert E\rvert$	Possible phases	Code*
5 6 10	2·47	45°	1
8 1 0	2·15	0	2
5 3 11	1·84	0	2
7 7 5	2·72	±45, ±135	3
6 6 10	2·16	±45, ±135	3

* 1 = origin and enantiomorph definition, 2 = origin definition, 3 = starting set.

Structure determination and refinement

Structure factors, after approximate scaling by application of Wilson's (1942) method, were converted into normalized structure amplitudes. The 294 larger E's ($E\ge 1{\cdot}20$) were used as input to the phase determination program *MULTAN* (Germain, Main & Woolfson, 1971), based on the weighted tangent formula. The program was used in its fully automatic mode, which yielded the choice of three origin-fixing reflexions (one of which was the enantiomorph) and two more reflexions as starting set (Table 2), with a probability threshold of 0·93. Out of the 16 possible solutions, the phases from the one with the greatest figure of merit (ABSFOM = 1·329) were chosen for a Fourier synthesis calculation. The map so obtained revealed all heavy atoms but a water molecule, the $R=\sum\lvert\lvert F_o\rvert-\lvert F_c\rvert\rvert/\sum\lvert F_o\rvert$ index being 0·37. Two full-matrix least-squares cycles with isotropic temperature parameters led to $R=0{\cdot}155$; at this stage in another Fourier map the still missing water oxygen was evident. Its contribution lowered R to 0·130 and a third isotropic least-squares cycle gave an R as low as 0·075. Two more least-squares cycles, still full-matrix and with introduction of anisotropic thermal parameters, gave $R=0{\cdot}035$. A difference Fourier synthesis at this stage gave indications for positioning all five hydrogen atoms. The last two least-squares cycles, all positional and thermal parameters (isotropic for hydrogen atoms) being varied at the same time as well as the scale factor, achieved convergence at $R=0{\cdot}027$ for the observed reflexions, and $R=0{\cdot}034$ including 'less thans'. A weight $1/\sqrt{\sigma}$, with σ derived from the counting statistics, was given to all observed reflexions.

No overall secondary extinction coefficient was applied, but during the very last cycles of refinement two reflexions (400 and 401) were excluded from calculations because they appeared to be affected by extinction.

The positional and isotropic thermal parameters, along with their standard deviations, are given in Table 3; anisotropic thermal parameters with their e.s.d.'s appear in Table 4.*

Table 3. *Atomic coordinates* ($\times 10^4$, *of the hydrogen atoms* $\times 10^3$) *and isotropic thermal parameters*

B's of the non-hydrogen atoms are the equivalent ones after Hamilton (1959).

	x/a	y/b	z/c	B (Å^2)
Na(1)	4715 (1)	6484 (2)	5000	2·56
Na(2)	2465 (1)	4734 (2)	1767 (2)	2·15
O(1)	998 (1)	5155 (2)	5492 (2)	1·22
O(2)	2931 (1)	5794 (2)	5942 (2)	1·05
O(3)	1663 (1)	1812 (2)	2904 (2)	1·22
O(4)	399 (1)	2024 (2)	4553 (2)	1·24
O(5)	2364 (1)	2664 (2)	4892 (2)	0·94
O(6)	2354 (1)	−4080 (2)	3933 (2)	1·18
O(7)	1723 (1)	−715 (2)	4511 (2)	1·07
OH(8)	−867 (2)	4314 (3)	5511 (2)	2·54
O(9)	2384 (2)	−1528 (3)	2542 (2)	1·57
O*W*(1)	5715 (2)	6639 (4)	7026 (3)	2·86
O*W*(2)	4772 (2)	7935 (6)	3045 (3)	4·74
B(1)	2165 (2)	4839 (4)	5064 (3)	0·82
B(2)	1568 (2)	1485 (4)	4217 (3)	0·89
B(3)	191 (2)	3792 (4)	5162 (3)	1·12
B(4)	2034 (2)	372 (4)	2135 (3)	0·80
B(5)	2141 (2)	−2086 (4)	3723 (2)	0·91
H(1)	−133 (2)	362 (4)	533 (3)	2·5 (7)
H(2)	569 (3)	791 (7)	666 (4)	8·5 (12)
H(3)	532 (3)	663 (7)	757 (4)	6·0 (14)
H(4)	418 (3)	786 (7)	271 (4)	7·8 (13)
H(5)	524 (4)	828 (7)	264 (4)	9·1 (14)

The solution of the structure gave unquestionable confirmation of the 2:5:5 molar ratio in nasinite, as well as its individualization among sodium borates.

Description of the structure and discussion

In spite of the noticeable difference in ionic radii of Na and K, the crystal structure of nasinite is directly related to that of the artificial $K_2[B_5O_8(OH)].2H_2O$ (Marezio, 1969). The difference is a slight rearrangement of the whole structure.

---

* A list of structure factors has been deposited with the British Library Lending Division as Supplementary Publication No. SUP 31038 (2 pp.). Copies may be obtained through The Executive Secretary, International Union of Crystallography, 13 White Friars, Chester CH1 1NZ, England.

The basic unit in the structure is the boron–oxygen polyion $[B_5O_8(OH)]^{2-}$ formed by two tetrahedra and three triangles in the shape of a double hexagonal ring. Tables 5 and 6 report bond distances and angles, as well as the B–O–B angles; in Table 7 all edges of boron polyhedra are compared and averaged. The average B–O distance in tetrahedra is 1·475 Å, in triangles 1·365 Å. The average O–O edge of the tetrahedra is 2·408 Å and that of triangles 2·363 Å. The two six-membered B–O rings are almost perpendicular to each other; an appreciable tilt from their planes is shown by the B–O triangles (Table 8). The mean B–B distances are 2·477 and 2·460 Å in rings 1 and 2 respectively, while the B–B inter-ring distances are: $B(1)–B(4^{x}) = 2{\cdot}529(4)$ Å and $B(1)–B(5) = 2{\cdot}503(4)$ Å; these values compare well with those given by Konnert, Clark & Christ (1972).

The polyion, with three triangles and two tetrahedra, has the same shape as the one found in ezcurrite (Cannillo, Dal Negro & Ungaretti, 1973); the $[B_5O_7(OH)_3]^{2-}$ polyion of the latter has three of its corners as OH groups. The same basic polyion shape was found in the sheet structures of veatchite (Clark & Christ, 1971), of p-veatchite (Rumanova & Gandymov, 1971), and of biringuccite (Corazza, Menchetti & Sabelli, 1974). Exactly the same polyion was found in gowerite (Konnert, Clark & Christ, 1972) and in the cited $K_2[B_5O_8(OH)].2H_2O$ (Marezio, 1969).

The structure is dominated by the boron-oxygen polymers; cations play a 'filling' rather than a leading role, though they have their own three-dimensional framework. Polymerization of the fundamental polyions into sheets takes place parallel to the **bc** plane through the linkage of polyions into chains along [010], and the two-dimensional bridging of the chains along [001].

The only OH group in the polyion protrudes alternately on both sides of the sheet, which attains a tip-to-tip thickness of more than $\frac{3}{4}a$ (9·4 Å approximately). Fig. 1 gives an overall view of the sheet conformation and relationships among polyions. Fig. 2(*a*) is an edge-on view of the unit cell, drawn in the same way as Marezio's (1969) Fig. 1. The two sheets in the cell are stacked along **a**, their symmetry being through the *n*

Table 5. Na–O *and* B–O *bond distances* (Å)

$Na(1)–O(1^{i})$	2·735 (2)	B(1)–O(1)	1·495 (3)
Na(1)–O(2)	2·429 (2)	B(1)–O(2)	1·482 (3)
$Na(1)–O(4^{ii})$	2·480 (2)	B(1)–O(5)	1·450 (3)
$Na(1)–O(6^{iii})$	3·099 (2)	$B(1)–O(6^{iii})$	1·465 (3)
$Na(1)–O(7^{iii})$	2·524 (2)	Mean	1·473
$Na(1)–OH(8^{i})$	2·884 (2)		
Na(1)–O*W*(1)	2·565 (3)	B(2)–O(3)	1·487 (4)
Na(1)–O*W*(2)	2·381 (3)	B(2)–O(4)	1·496 (3)
Mean	2·637	B(2)–O(5)	1·440 (3)
		B(2)–O(7)	1·482 (3)
$Na(2)–O(2^{iv})$	2·769 (2)	Mean	1·476
Na(2)–O(3)	2·483 (2)		
$Na(2)–O(5^{v})$	2·842 (2)	B(3)–O(1)	1·366 (3)
$Na(2)–O(6^{iii})$	2·544 (3)	B(3)–O(4)	1·361 (3)
$Na(2)–O(7^{v})$	2·719 (3)	B(3)–OH(8)	1·372 (3)
$Na(2)–OH(8^{vi})$	2·458 (3)	Mean	1·366
$Na(2)–O(9^{vii})$	2·588 (2)		
$Na(2)–OW(1^{viii})$	2·380 (3)	$B(4)–O(2^{iv})$	1·361 (3)
Mean	2·598	B(4)–O(3)	1·348 (3)
		B(4)–O(9)	1·384 (3)
		Mean	1·364
		B(5)–O(6)	1·345 (3)
		B(5)–O(7)	1·351 (3)
		B(5)–O(9)	1·399 (3)
		Mean	1·365

The key to the symmetry operations, used in this and in the following tables, is:

Superscript			
None	x	y	z
i	$\frac{1}{2}+x$	$\frac{3}{2}-y$	z
ii	$\frac{1}{2}+x$	$\frac{1}{2}-y$	z
iii	x	$y-1$	z
iv	$\frac{1}{2}-x$	$y-\frac{1}{2}$	$z-\frac{1}{2}$
v	$\frac{1}{2}-x$	$\frac{1}{2}+y$	$z-\frac{1}{2}$
vi	$-x$	$1-y$	$z-\frac{1}{2}$
vii	x	$1+y$	z
viii	$1-x$	$1-y$	$z-\frac{1}{2}$
ix	x	$y-1$	z
x	$\frac{1}{2}-x$	$\frac{1}{2}+y$	$\frac{1}{2}+z$
xi	$x-\frac{1}{2}$	$\frac{1}{2}-y$	z

Table 4. *Heavy-atom thermal parameters* ($\times 10^5$) *in the form* $T = exp\,[-(\beta_{11}h^2+\beta_{22}k^2+\beta_{33}l^2+2\beta_{12}hk+2\beta_{13}hl+2\beta_{23}kl)]$

	β_{11}	β_{22}	β_{33}	β_{12}	β_{13}	β_{23}
Na(1)	403 (8)	1403 (27)	595 (10)	102 (13)	174 (8)	192 (15)
Na(2)	411 (7)	1066 (23)	453 (9)	56 (12)	−42 (7)	12 (14)
O(1)	174 (10)	589 (35)	332 (13)	−26 (15)	29 (10)	−182 (19)
O(2)	235 (11)	524 (36)	179 (11)	−91 (16)	−38 (10)	24 (17)
O(3)	359 (12)	478 (33)	154 (11)	115 (17)	−7 (10)	11 (16)
O(4)	170 (10)	652 (34)	327 (13)	−24 (16)	18 (10)	−143 (19)
O(5)	170 (9)	381 (30)	241 (11)	8 (14)	−34 (9)	−6 (18)
O(6)	340 (12)	446 (32)	166 (11)	67 (16)	18 (10)	0 (16)
O(7)	291 (11)	386 (32)	177 (11)	4 (16)	24 (10)	17 (17)
OH(8)	172 (11)	1406 (49)	847 (21)	−57 (19)	74 (13)	−697 (29)
O(9)	470 (14)	602 (35)	192 (12)	223 (19)	97 (11)	91 (19)
O*W*(1)	466 (15)	1706 (56)	601 (20)	89 (25)	200 (15)	288 (30)
O*W*(2)	427 (19)	4958 (124)	668 (23)	−78 (40)	−55 (18)	798 (47)
B(1)	164 (14)	388 (48)	172 (17)	−14 (22)	−24 (14)	−11 (26)
B(2)	202 (15)	419 (47)	156 (16)	24 (23)	1 (14)	−7 (24)
B(3)	190 (16)	652 (52)	231 (19)	14 (25)	10 (14)	−26 (28)
B(4)	111 (13)	468 (49)	195 (17)	−2 (23)	−9 (14)	16 (26)
B(5)	173 (15)	531 (54)	169 (18)	15 (23)	−16 (14)	15 (26)

glide plane. The bonds between adjacent sheets take place *via* one direct H bond and the Na polyhedra. The protruding hexagonal rings of each sheet are accomodated in front of the flat portion of the adjacent sheet, thus allowing an inter-sheet spacing of $\frac{1}{2}a$.

Both Na atoms exhibit an eightfold coordination, Na–O distances ranging from 2·380 to 3·099 Å; the average Na–O distance is 2·618 Å. Coordination polyhedra are quite irregular in shape; the Na(1) polyhedron resembles an octahedron with two opposite corners split in the same direction, in a position approximately midway between the B–O sheets. Atom Na(2) lies instead within the B–O sheet, filling the 'holes' with trigonal symmetry, which are evident in Fig. 1. Its coordination polyhedron is comparable with a hexagonal bipyramid. Both Na(1) and Na(2) provide the links between adjacent sheets as well as with the water molecules. The Na(1) polyhedron shares two of its edges with two neighbouring Na(2) polyhedra, thus building up zigzag chains in the **a** direction. In turn each of these chains is connected to the four surrounding it, alternately in the **bc** diagonals. The resulting three-dimensional Na–O network has a condensation along the chains. Fig. 2(*b*) depicts the Na–O bonds.

The two water molecules lie in the gaps between the sheets; O*W*(1) is bound to both Na atoms, O*W*(2) to Na(1) only. They make hydrogen bonds with the surrounding oxygen atoms: O*W*(1) with oxygens of different sheets, O*W*(2) with those within the same sheet. Distances and angles relating to the hydrogen bonds are given in Table 9. Unlike potassium pentaborate dihydrate, described by Marezio (1969), the

Table 6. *Bond angles around the boron atoms in the tetrahedra and triangles, and* B–O–B *angles* (°)

O(1)–B(1)–O(2)	108·2 (2)
O(1)–B(1)–O(5)	109·3 (2)
O(1)–B(1)–O(6^{iii})	110·8 (2)
O(2)–B(1)–O(5)	113·2 (2)
O(2)–B(1)–O(6^{iii})	105·8 (2)
O(5)–B(1)–O(6^{iii})	109·3 (2)
O(3)–B(2)–O(4)	106·6 (2)
O(3)–B(2)–O(5)	112·9 (2)
O(3)–B(2)–O(7)	110·4 (2)
O(4)–B(2)–O(5)	111·5 (2)
O(4)–B(2)–O(7)	106·8 (2)
O(5)–B(2)–O(7)	108·5 (2)
O(1)–B(3)–O(4)	123·7 (2)
O(1)–B(3)–OH(8)	114·8 (2)
O(4)–B(3)–OH(8)	121·5 (2)
O(2^{iv})–B(4)–O(3)	119·6 (2)
O(2^{iv})–B(4)–O(9)	119·6 (2)
O(3)—B(4)–O(9)	120·9 (2)
O(6)–B(5)–O(7)	126·5 (2)
O(6)–B(5)–O(9)	112·1 (2)
O(7)–B(5)–O(9)	121·4 (2)
Ring 1	
B(1)–O(5)–B(2)	118·8 (2)
B(2)–O(4)–B(3)	119·8 (2)
B(3)–O(1)–B(1)	119·3 (2)
Ring 2	
B(2)–O(7)–B(5)	122·8 (2)
B(5)–O(9)–B(4)	118·6 (2)
B(4)–O(3)–B(2)	123·7 (2)
Inter-ring	
B(1)—O(2)–B(4^{x})	125·6 (2)
B(1^{iii})–O(6)–B(5)	125·9 (2)

Table 7. *The* O–O *edges of the boron coordination polyhedra*

B(1) tetrahedron		B(3) triangle	
O(1)···O(2)	2·413 (2) Å	O(1)···O(4)	2·405 (2) Å
O(1)···O(5)	2·404 (2)	O(1)···OH(8)	2·307 (2)
O(1)···O(6^{iii})	2·436 (3)	O(4)···OH(8)	2·384 (3)
O(2)···O(5)	2·450 (2)	Mean	2·365
O(2)···O(6^{iii})	2·351 (3)		
O(5)···O(6^{iii})	2·378 (2)	B(4) triangle	
Mean	2·405	O(2)–O(3^{x})	2·341 (3)
		O(2)–O(9^{x})	2·373 (3)
B(2) tetrahedron		O(3)–O(9)	2·378 (2)
O(3)···O(4)	2·392 (3)	Mean	2·364
O(3)···O(5)	2·440 (2)		
O(3)···O(7)	2·438 (3)	B(5) triangle	
O(4)···O(5)	2·427 (2)	O(6)···O(7)	2·409 (2)
O(4)···O(7)	2·392 (2)	O(6)···O(9)	2·276 (3)
O(5)···O(7)	2·371 (2)	O(7)···O(9)	2·398 (3)
Mean	2·410	Mean	2·361

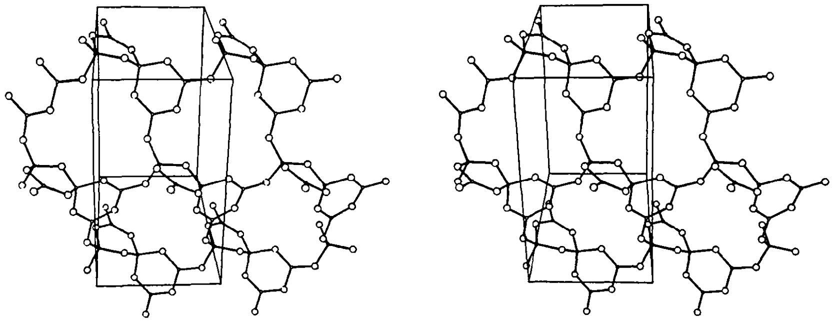

Fig. 1. A stereoscopic illustration of one B–O sheet seen along [100]. Spheres are of arbitrary size. The origin is in the lower left foreground, **b** is to the right and **c** to the top of the page, **a** is pointing into the page. The plotting program *ORTEP* (Johnson, 1965) was used for both this figure and Fig. 2.

two water molecules in nasinite make no H bond with each other. The O*W*(1)···O*W*(2) distance is 3·243(5) Å, while in Marezio's (1969) K borate it is 3·02 Å. On the other hand, in nasinite an O*W*(2)···OH(8) distance of 3·249(4) Å is found (3·30 Å in Marezio, 1969). Though in the K borate structure there was no doubt in assigning the H bond to the O*W*(1)···O*W*(2) distance, in nasinite the two possible distances are quite similar; all indications (ΔF map, trend of refinement, charge balance) have been for the O*W*(2)··· OH(8) possibility, yet this H bond is very weak. The hydrogen bond provided by H(3), belonging to O*W*(1), has been found to be most likely bifurcated (both because of distances and angles and because of its position) in the same way as in Marezio's (1969) structure.

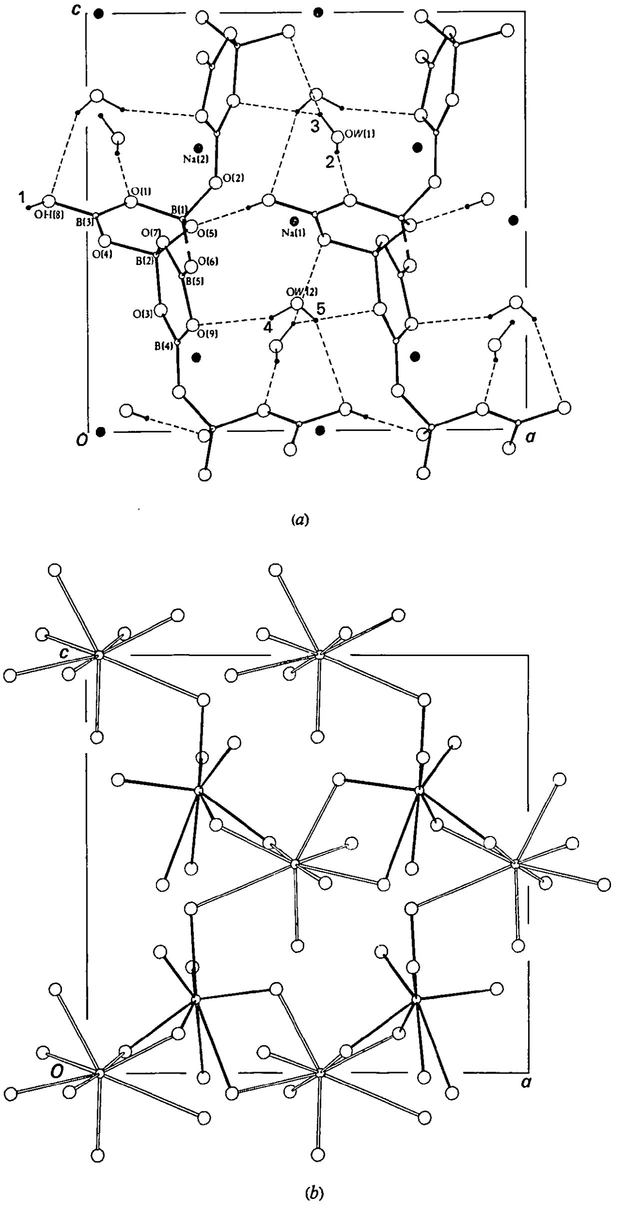

(*a*)

(*b*)

Fig. 2. (*a*) The **ac** projection (right-handed) of the unit cell, drawn for comparison in the same way as Marezio's (1969) Fig. 1 and showing atomic nomenclature. Broken lines represent hydrogen-acceptor bonds. (*b*) The same projection showing the framework of the Na–O bonds. Differentiation is made by blackening Na(2) bonds.

Because of the zeolitic character of the water molecules both in nasinite and in K pentaborate dihydrate, the dehydration dynamics exhibited by the latter are very likely to occur in the analogous sodium compounds. This can be inferred also by comparison of the values given in Table 9 with those of Marezio (1969).

An electrostatic valence balance was calculated according to the method given by Brown & Shannon (1973) with constants from their Table 1, using for hydrogen bonds the curve calculated by the same authors and reported by Donnay & Donnay (1973). Table 10 reports the contributions of different atoms and the bond-strength sums (v.u.). From these results a confirmation of the bond system, and especially of the H bonds, results. Only two oxygen atoms do not exhibit fourfold coordination: O*W*(2) has a coordination number of 3 [Na(1)+its H's], and OH(8) coordinates five neighbours, two of which however give a very weak contribution.

The computational programs used throughout this work and adapted for the CII 10070 computer are the *MULTAN* program by Germain, Main & Woolfson (1971), the *ORFLS* least-squares program by Busing, Martin & Levy (1962), *ORTEP* plot program by Johnson (1965), *BONDLA* and *LSQPL* programs for the X-RAY System by Stewart, Kruger, Ammon, Dickinson & Hall (1972).

References

Brown, J. D. & Shannon, R. D. (1973). *Acta Cryst.* A**29**, 266–282.

Busing, W. R., Martin, K. O. & Levy, H. A. (1962). *ORFLS*. Oak Ridge National Laboratory Report ORNL-TM-305.

Cannillo, E., Dal Negro, A. & Ungaretti, L. (1973). *Amer. Min.* **58**, 110–115.

Cipriani, C. (1961). *Atti Accad. Nazl. Lincei. Rend. Classe Sci. Fis. Mat. Nat.* **30**, 235–245.

Cipriani, C. & Vannuccini, P. (1961). *Atti Accad. Nazl. Lincei. Rend. Classe Sci. Fis. Mat. Nat.* **30**, 74–83.

Clark, J. R. & Christ, C. L. (1971). *Amer. Min.* **56**, 1934–1954.

Corazza, E., Menchetti, S. & Sabelli, C. (1974). *Amer. Min.* **59**, 1005–1015.

Donnay, G. & Donnay, J. D. H. (1973). *Acta Cryst.* B**29**, 1417–1425.

Germain, G., Main, P. & Woolfson, M. M. (1971). *Acta Cryst.* A**27**, 368–376.

Hamilton, W. C. (1959). *Acta Cryst.* **12**, 609–610.

Johnson, C. K. (1965). *ORTEP*. Oak Ridge National Laboratory Report ORNL-3794.

Karle, I. L., Dragonette, K. S. & Brenner, S. A. (1965). *Acta Cryst.* **19**, 713–716.

Table 8. *Displacements of other atoms from the planes of ring oxygens; dihedral angles in the polyion*

	Ring 1		Ring 2	
Ring oxygen atoms	O(1), O(4), O(5)		O(3), O(7), O(9)	
Associated atoms	B(1)	−0·43 Å	B(2)	0·20 Å
	B(2)	−0·28	B(4)	−0·11
	B(3)	0·12	B(5)	−0·05
	O(2)	0·11	O(2)	−0·32
	O(3)	−1·69	O(4)	−0·88
	O(6)	−1·89	O(5)	1·51
	O(7)	0·63	O(6)	−0·17
	OH(8)	0·41		
Angle between rings	83·4°			
Oxygen atoms of triangle	O(1), O(4), OH(8)		O(2), O(3), O(9)	
Triangle–ring angle	11·7°		9·1°	
Oxygen atoms of triangle			O(6), O(7), O(9)	
Triangle–ring angle			4·7°	

Table 9. *Hydrogen-bonding system with related distances* (Å) *and angles* (°)

Donor atom (D)	H	Acceptor atom (A)	$D\cdots A$	D–H	H$\cdots A$	D–H$\cdots A$	H–D–H	$A\cdots D\cdots A$
OH(8)	H(1)	$O(5^{xi})$	2·580 (2)	0·75 (3)	1·84 (3)	169 (3)		
OW(1)	H(2)	$O(1^{i})$	2·724 (3)	0·92 (4)	1·86 (4)	156 (4)		
OW(1)	H(3)	$O(3^{x})$	3·022 (3)	0·78 (5)	2·41 (4)	137 (4)	110 (4)	107·08 (9)
		$O(4^{x})$	3·134 (4)		2·39 (5)	162 (4)	$AHA=60$ (1)	123·98 (10)
OW(2)	H(4)	$O(9^{vii})$	2·944 (3)	0·80 (4)	2·21 (4)	153 (4)		
OW(2)	H(5)	$OH(8^{v})$	3·249 (4)	0·72 (4)	2·60 (5)	151 (4)	111 (5)	101·29 (10)

Table 10. *The electrostatic valence balance*

	Na(1)	Na(2)	B(1)	B(2)	B(3)	B(4)	B(5)	H_{don}	H_{acc}	Sums
O(1)	0·09		0·71		1·00				0·21	2·01
O(2)	0·17	0·08	0·73			1·01				1·99
O(3)		0·15		0·73		1·05			0·07	1·99
O(4)	0·16			0·71	1·02				0·06	1·95
O(5)		0·07	0·80	0·82					0·26	1·95
O(6)	0·04	0·14	0·76				1·05			2·00
O(7)	0·14	0·09		0·74			1·04			2·01
OH(8)	0·07	0·16			0·98			0·74	0·05	2·00
O(9)		0·12				0·94	0·91		0·16	2·13
OW(1)	0·13	0·19						0·79 0·87		1·98
OW(2)	0·20							0·84 0·95		1·99
Sums	1·00	1·00	3·00	3·00	3·00	3·00	3·00	4·19	0·81	22·00

Konnert, J. A., Clark, J. R. & Christ, C. L. (1972). *Amer. Min.* **57**, 381–396.

Marezio, M. (1969). *Acta Cryst.* B**25**, 1787–1795.

Milman, T. & Bouaziz, M. R. (1965). *Bull. Soc. Chim. Fr.* pp. 7–13.

Nies, N. P. & Erd, R. C. (1963). Cited in Erd, R. C. (1963). *Amer. Min.* **48**, 709–711.

Nies, N. P. & Hulbert, R. W. (1967). *J. Chem. Eng. Data*, **12**, 303–313.

Rumanova, I. M. & Gandymov, O. (1971). *Sov. Phys. Cryst.* **16**, 75–81.

Stewart, J. M., Kruger, G. J., Ammon, H. L., Dickinson, C. & Hall, S. R. (1972). The X-RAY System. Computer Science Center, Univ. of Maryland.

Stoppioni, A. (1974). Thesis, Univ. Firenze, Italy.

Tennyson, C. (1963). *Fortschr. Miner.* **41**, 64–91.

Wilson, A. J. C. (1942). *Nature, Lond.* **150**, 151–152.